

## SUBSTRATE THICKNESS EFFECT ON THE INTEGRATED INTERLEAVED TRANSFORMER IN RF

Namoune ABDELHADI<sup>1\*</sup>, Melati RABIA<sup>2</sup>, Benzidane Mohammed RIDHA<sup>3</sup>,  
Pierre SPITERI<sup>4</sup>, Abdelkader BOUKORTT<sup>5</sup>

*This article presents two aspects of research into improving the performance of integrated trans-former. The first aspect represents the effect substrate thickness on micro transformer properties. Interleaved structure is simulated using the MATLAB simulator, these results illustrate that improved performance of the interleaved transformer is dependent on increasing the thickness of substrate. However, increasing thickness of the substrate past certain limit does not contribute to improvement of performance the transformer. Second aspect, A study our transformer in terms of thermal behavior and electromagnetic to improviser the performance of the transformer, by using COMSOL Multiphysics 5.3 software, this result illustrates the electrical potential, the current density and the temperature distribution.*

**Keywords:** Integration, Interleaved transformer, Substrate thickness, RF

### 1. Introduction

Radio Frequency (RF) Direct Current (DC) converters are critical components of many electronic devices, including wireless communication systems, radar systems, and medical devices [1][2]. However, one of the major challenges in designing RF DC-DC converters is managing the heat generated during their operation. Temperature rise can negatively impact the performance of RF components, such as transistors, and result in energy losses [3][4].

To address this issue, researchers have explored various approaches to reducing thermal effects and losses in RF circuits, including the use of a thin substrate [5]. A thin substrate facilitates the evacuation of heat flow, reducing

<sup>1</sup> Department of Electrotechnical & Automatic Engineering, Relizane University, Algeria. e-mail: abdelhadi.namoune@cu-relizane.dz

<sup>2</sup> Laboratory of Applied Power Electronic (LEPA), University of Sciences and Technology of Oran (USTO-MB), Oran, Algeria, e-mail: mel\_ati@hotmail.fr

<sup>3</sup> Laboratoire d'Elaboration Caractérisation Physico Mécanique et Métallurgique des Matériaux (ECP3M), Electrical Engineering Department, Abdelhamid Ibn Badis University, Mostaganem, Algeria, e-mail: ridha.benzidane.etu@univ-mosta.dz

<sup>4</sup> INP-ENSEEIHT, IRIT, Toulouse, France, e-mail: pierre.spiteri@toulouse-inp.fr

<sup>5</sup> Laboratoire d'Elaboration Caractérisation Physico Mécanique et Métallurgique des Matériaux (ECP3M), Electrical Engineering Department, Abdelhamid Ibn Badis University, Mostaganem, Algeria., e-mail: abdelkader.boukort@univ-mosta.dz

thermal resistance and improving heat dissipation. However, using a very thin substrate can affect the performance of components due to electromagnetic flux [6], such as a decrease in the coupling coefficient (K) and quality factor (Q) of the RF transformer [7]. Consequently, this results in decreased energy efficiency and increased energy loss [8][9]. The integrated interleaved transformer is a key component in DC-DC converters, providing voltage conversion and isolation [10]. Therefore, it is essential to optimize its performance for efficient and reliable operation of the converter. In this paper, we investigate the influence of substrate thickness on the performance of integrated interleaved transformers in RF circuits.

Our analysis considers the electromagnetic and thermal behavior of a micro-transformer, taking into account substrate thickness. We examine the impact of substrate thickness on the coupling coefficient and quality factor of the transformer, as well as its energy efficiency and energy loss. We also explore the effect of substrate thickness on the thermal behavior of the transformer. Through our research, we aim to provide insights into the optimal substrate thickness for integrated interleaved transformers in RF circuits. Our findings can help designers of RF DC-DC converters to improve their performance, reduce energy losses, and enhance their reliability. To achieve our objectives, we used a combination of analytical measurements, electromagnetic simulations, and thermal modeling. We investigated a series of micro-transformers with different substrate thicknesses and characterized their electrical behavior. We then opted the optimal geometry and simulated the performance of the transformers using electromagnetic and thermal analysis tools and validated our findings.

In summary, this paper investigates the impact of substrate thickness on the performance of integrated interleaved transformers in RF circuits. By exploring the electromagnetic and thermal behavior of micro-transformers, we provide a better understanding of how to optimize the design of RF DC-DC converters. this research can contribute to the development of more efficient, reliable, and cost-effective RF DC-DC converters.

## **2. Geometric parameters of the interleaved transformer**

The structure of the interleaved transformer has several physical layout parameters, which also have an impact on its performance, and they are as follows: ratio turn (a), spacing between turns (S), width of metal (W), thickness of metal (d) and the external diameter (D), as shown in Fig. 1. The values of these parameters are given in Table 1.

The interleaved transformer uses the same metal layer. The  $N_p$  and  $N_s$  are sideways interleaved. The coupling is weak when the distance between two turns is greater than the width of two successive metallic layers. However, the

interleaved construction attains high symmetry, which makes the phase difference between the differential signals slightly [11] [12].

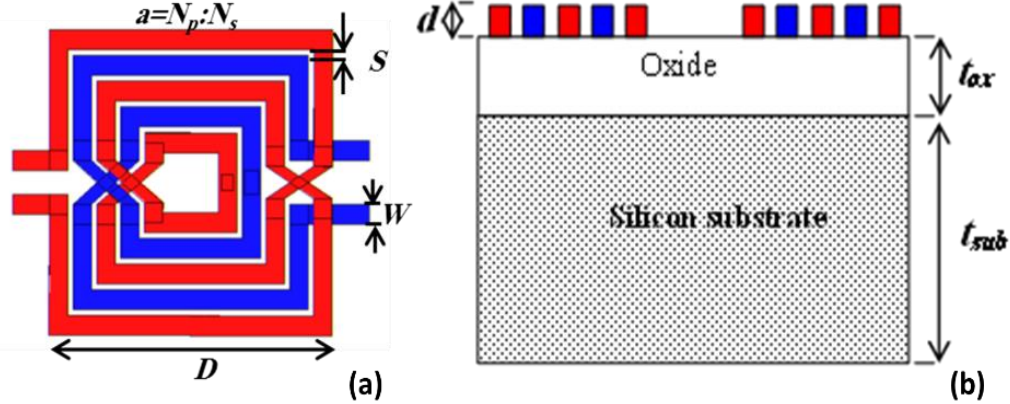


Fig. 1. Layout parameters (a) Physical layout, (b) Cross-sectional view of the on-silicon interleaved transformer

Table 1

Gathers the values of the geometric parameters.

Parameter	Symbol	Value
Outer diameter	D	280 $\mu\text{m}$
Conductor width	W <sub>p</sub> =W <sub>s</sub> =W	20 $\mu\text{m}$
Metal spacing	S	10 $\mu\text{m}$
Metal thickness	d	12 $\mu\text{m}$
Number of turns	N <sub>p</sub> : N <sub>s</sub>	3 : 2
Thickness of oxide	t <sub>ox</sub>	25 $\mu\text{m}$
Thickness of substrate	t <sub>sub</sub>	100 $\mu\text{m}$

### 3. Lumped-Element Model

The coupling of two inductors forms a transformer. Fig. 2 shows a simple  $\pi$ -network for modeling a single inductor, containing the series resistance (R<sub>s</sub>) due to skin effect, series inductance (L<sub>s</sub>) due to the magnetic flux, The capacitors oxide (C<sub>ox1</sub> and C<sub>ox2</sub>) represents the capacitances parasitic between substrate and metal coils, the capacitances parasitic substrate (C<sub>sub</sub>) and resistance substrate (R<sub>sub</sub>) [13].

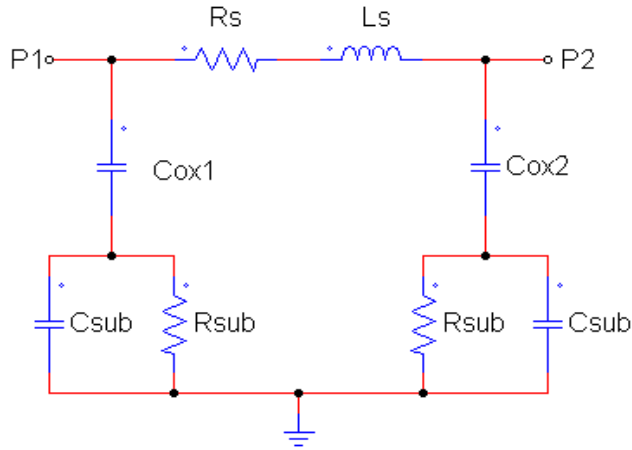


Fig. 2. The  $\pi$ -network of a spiral inductor [15]

The resistance (R) and inductance (L) of the inductor in the substrate are extracted by Y-parameters in Equation (1) and (2), respectively [14] [15]. To reduce the energy loss, we also extract the quality factor expressed in the Equation. (3) [16] [17].

$$L = \frac{\text{Imag}(1/Y_{11})}{2\pi f} \quad (1)$$

$$R = \text{Real}(-1/Y_{11}) \quad (2)$$

$$Q = \frac{\text{Imag}(1/Y_{11})}{\text{Real}(1/Y_{11})} \quad (3)$$

Fig. 3 shows a lumped-element model of the transformer when the two windings are coupled using the  $\pi$ -network model [18]. Which includes the following items: ( $R_p$  and  $R_s$ ), ( $L_p$  and  $L_s$ ) represents resistance and inductance of primary and secondary coils respectively, the capacitance coupling between  $N_p$  and  $N_s$  ( $C_{p1}$  and  $C_{p2}$ ), the capacitors oxide ( $C_{ox1}$  and  $C_{ox2}$ ), the capacitances parasitic substrate ( $C_{sub}$ ) and resistance substrate ( $R_{sub}$ ). Transformer power-efficiency is affected by substrate losses [19] [20].

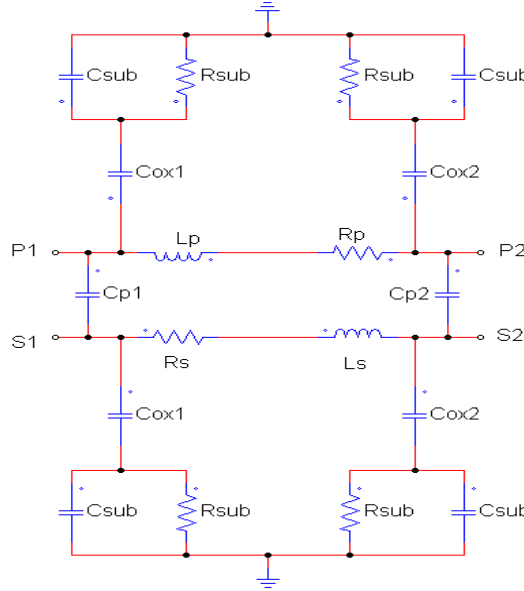


Fig. 3. The lumped-element model of a transformer

The coupling coefficient ( $K$ ) is extracted from Z-parameters and expressed in Equation (4). Which converts the power from the primary coils to the secondary coils and shows its amount [21].

$$K = \left( \frac{\text{Imag}(Z_{12}) * \text{Imag}(Z_{21})}{\text{Imag}(Z_{11}) * \text{Imag}(Z_{22})} \right)^{1/2} \quad (4)$$

#### 4. Study of performances of the transformer for different substrate thicknesses

In planar structures, a semiconductor substrate is used as a support and heat flow evacuator. To know the impact of the substrate thickness on the operating of the interleaved transformer, we carried out different simulations. The simulations are carried out using MATLAB software for different substrate thicknesses (20 $\mu\text{m}$ , 100 $\mu\text{m}$ , 125 $\mu\text{m}$  and 150 $\mu\text{m}$ ).

At the default substrate thickness of 150  $\mu\text{m}$ , Fig. 4(a) illustrates the variation of  $L_p$  as a function of frequency. The value of the self-resonant frequency is 6.7GHz for the three  $T_{\text{sub}}$  values (100 $\mu\text{m}$ , 125 $\mu\text{m}$  and 150 $\mu\text{m}$ ), and increases to 8.3GHz when  $T_{\text{sub}}$  is reduced to 20 $\mu\text{m}$ . We note that as the thickness of the substrate  $T_{\text{sub}}$  decreases, the  $L_p$  decreases as well. This could be explained due to the high value of parasitic capacitance created for the transformer with 20 $\mu\text{m}$  substrate, which permits more leakage current to flow through the substrate. The increased leakage current could result in a greater loss of energy, affecting the behavior of the transformer and leading to a lower inductance. Therefore, the

thinner substrate leads to a different behavior compared to the other three substrates, as evidenced by the change in self-resonant frequency and the decrease in inductance.

Fig. 4(b) shows the variation of primary coil resistance ( $R_p$ ) as a function of frequency with different substrate thicknesses ( $T_{sub}$ ). The curves of primary coil resistance versus frequency are nearly the same when the thickness of substrate ( $T_{sub}$ ) vary from 100  $\mu\text{m}$  to 150  $\mu\text{m}$ . When the thickness of substrate decreases to 10  $\mu\text{m}$ , the curve varies towards higher frequency.

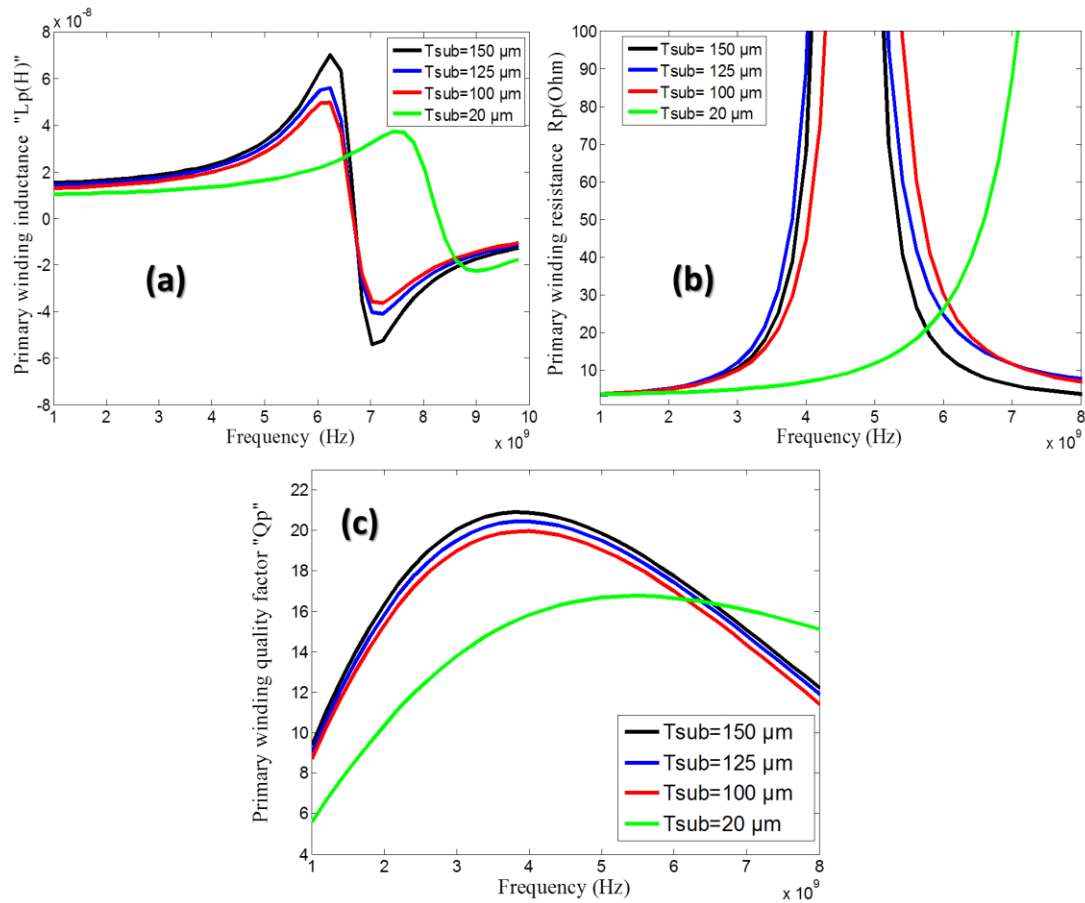


Fig. 4. Variations (a)  $L_p$  , (b)  $R_p$  and (c)  $Q_p$  as a function of frequency with different substrate thickness ( $T_{sub}$ )

Fig. 4(c) shows the variance of primary quality factor ( $Q_p$ ) as a function of frequency with different substrate thickness ( $T_{sub}$ ). At 3.8 GHz, the quality factor achieves a maximum value of 21 for  $T_{sub} = 150 \mu\text{m}$  and then decreases to 20 when the  $T_{sub} = 100 \mu\text{m}$ . As for the thickness of substrate 20  $\mu\text{m}$ , the maximum value of quality factor is 16.8 at frequency 5.5 GHz. A decrease the resistance of 20  $\mu\text{m}$

substrate causes a decrease of metal loss. However, the magnetic power dissipation of the substrate increases, which reduces the quality factor.

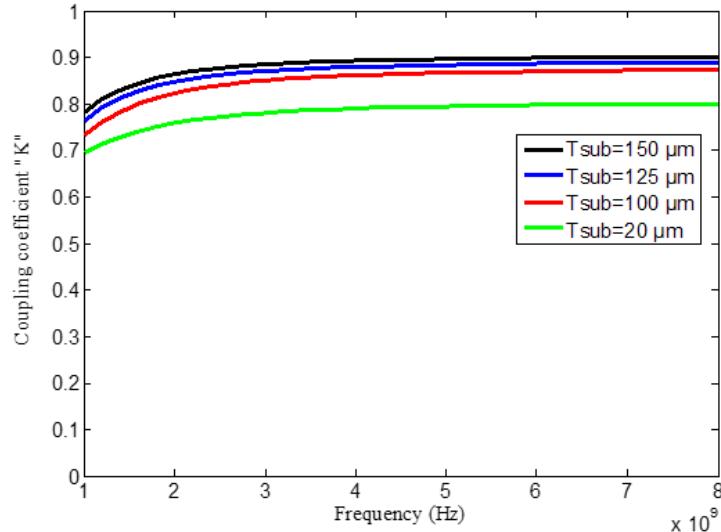


Fig. 5. Variation of K as a function of frequency with different substrate thickness.

By equation (4), Fig. 5 shows the variation of coupling coefficient (K) as a function of frequency with different substrate thicknesses (Tsub). A high coupling coefficient (K) signify a good energy conversion from primary to the secondary coils. There is high affinity of the coupling coefficients for substrates thicknesses following: 100  $\mu\text{m}$ , 125  $\mu\text{m}$  and 150  $\mu\text{m}$  at range 0.90. For a substrate thickness 20  $\mu\text{m}$ , the coupling coefficient drops to 0.8. The magnetic loss of the substrate rises due to decrease thickness of the substrate, which results a decrease magnetic power converted from primary coil to secondary coil.

#### 4.1 Result and discussion.

This study allowed us to see the impact of the substrate thickness on the operating of an interlaced transformer. We observed through different simulations that a very thin substrate thickness degrades the performance of the transformer.

The results obtained shown that the thickness of 20  $\mu\text{m}$  does not give the desired results, and that the three thicknesses (100  $\mu\text{m}$ , 125  $\mu\text{m}$ , and 150  $\mu\text{m}$ ) give a best quality factor and a great coupling factor, with a fairly high resonance frequency.

We opt for a substrate thickness of 100  $\mu\text{m}$  and we move on to the simulation of electromagnetic effects.

## 5. Simulation of electromagnetic effect

In this part, we use the COMSOL Multiphysics software to present an electromagnetic simulation on the interleaved transformer with a substrate thickness of 125  $\mu\text{m}$ . For good accuracy, we move on to a very fine triangular mesh. Fig. 6 show the 3D fine triangular mesh of an interleaved transformer structure.

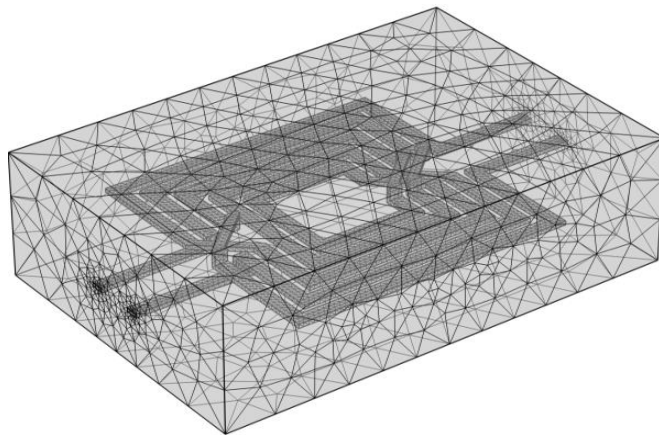


Fig.6. 3D mesh of 2-to-3 interleaved transformer

### 5.1 Electrical potential

Fig. 7 shows the distribution of the electrical potential in the interleaved transformer, we observe that the voltage of the primary is greater than that of the secondary because of  $(N_p/N_s) > 1$ .

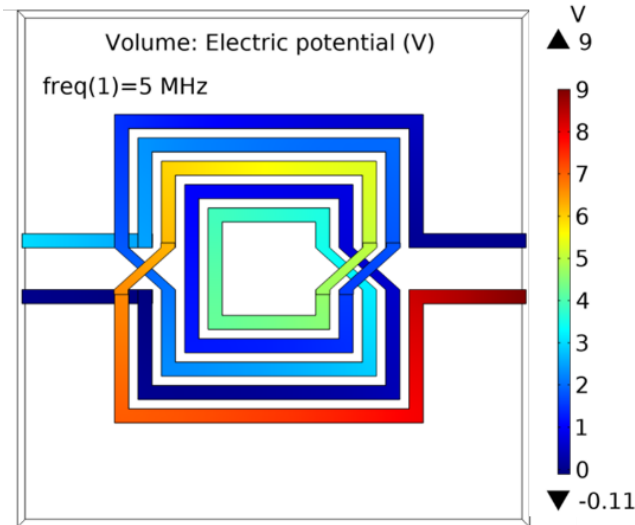


Fig.7. Distribution of the electrical potential in the interleaved transformer.

## 5.2 Current density

Fig. 8 illustrate the distribution of the current density in the interleaved transformer. We notice that the current density is almost evenly distributed in the primary winding, as well as the secondary, except for a very slight spike effect because of the inhomogeneous resistances in the conductor's angles. At the crossing of the two windings, the current density increases because of sections which decrease

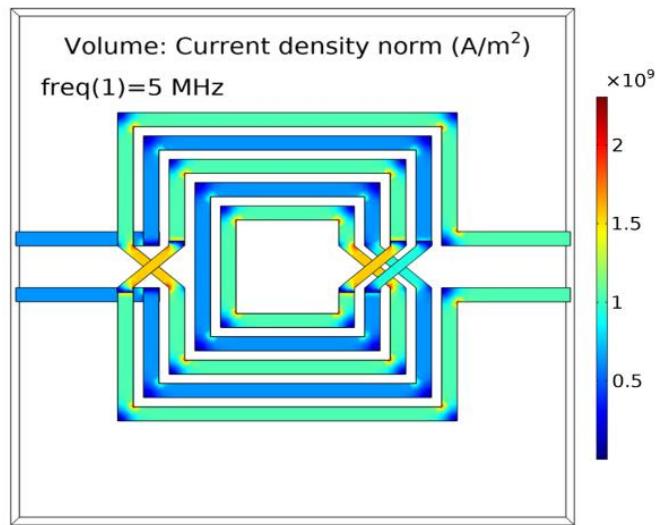


Fig.8. Current density in the interleaved transformer

Fig. 9 shows the current density inside the conductors. We notice the total absence of the skin effect; this is explained by the fact that the thickness ( $d$ ) and the width ( $W$ ) of the conductor are less than the skin thickness. The absence of the skin effect implies negligible losses by joule effects. We also notice that the current density in the secondary is greater than that of the primary, because of  $(N_p/N_s) > 1$  so, the intensity of the output current is greater than that of the input current.

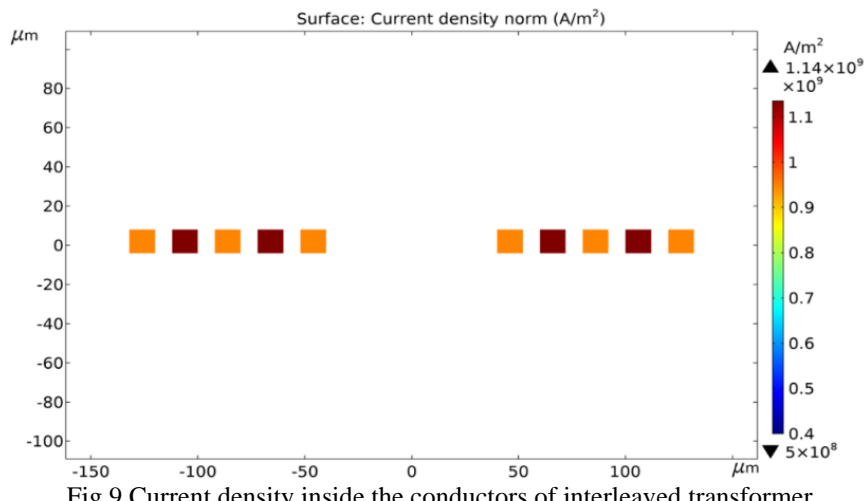


Fig.9.Current density inside the conductors of interleaved transformer

If we draw the curve of the current density according to the cross section shown in Fig. 10(a), we obtain Fig. 10(b).

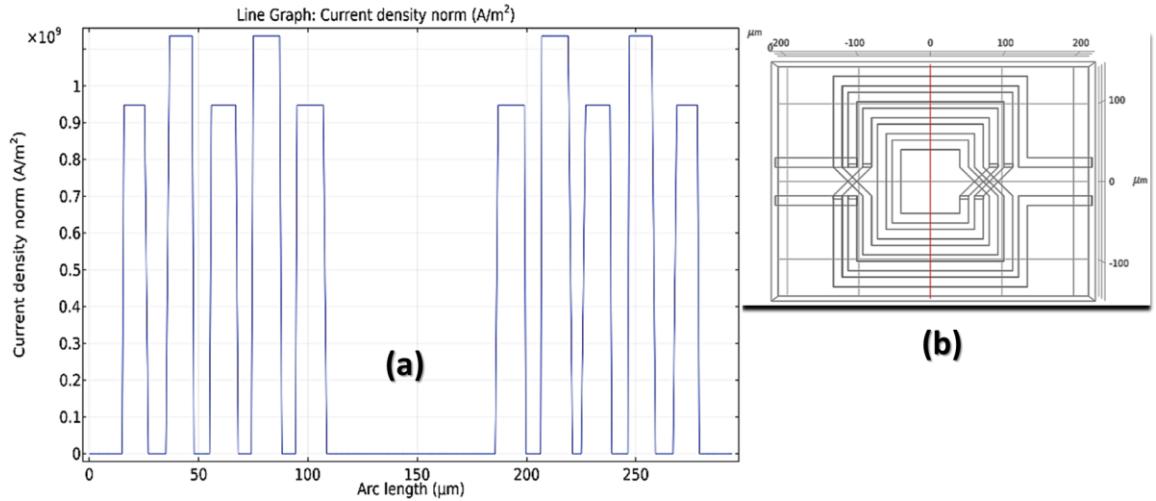


Fig.10. (a) Variation of current density in primary and secondary coils of interlaced transformer.  
(b) Cross section

Fig. 10(b) shows that the current density of the secondary ( $I_2 = 1.138 \cdot 10^9 \text{ A/m}^2$ ) is greater than that of the primary ( $I_1 = 0.947 \cdot 10^9 \text{ A/m}^2$ ) which gives a ratio  $(I_2/I_1) = 1.2$ . This ratio is slightly lower than  $(N_p/N_s)$  because of the energy losses. We see in this figure that the current density between the turns is almost zero, which allows us to say that the capacitive effect between turns is zero.

## 6. Temperature distribution in the interleaved transformer

### 6.1 Physical model

Using the COMSOL simulation software, we will study the temperature distribution in the different layers of the interlaced transformer, they are: the layer of the copper windings, the oxide insulating layer, and the layer of the silicon substrate. The physical model in 3D of interlaced transformer is shown in Fig. 11.

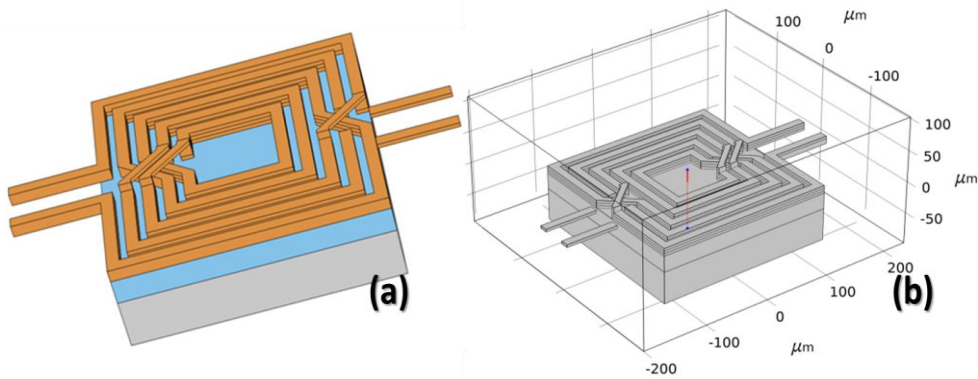


Fig.11. (a) The physical 3D model of interleaved transformer, (b) Boundaries and axis of the study domain

### 6.2 Mathematical model.

Thermal modeling consists in seeing the thermal behavior of the interleaved transformer in the face of a heat factor. The stationary analytical thermal model is a representation of the thermal behavior in the case of structures considered to be a solid, this modeling uses several transformations of mathematical functions such as (Kirchhoff, Fourier and Green) [22] [23] [24] to define the heat transfer Eqn. (5).

$$k\nabla^2T = \rho_n CP_n \left( \frac{\partial T}{\partial t} \right) + Q \quad (5)$$

Since the transformer is made of different materials, the heat equation becomes:

$$\rho_i CP_i \left( \frac{\partial T}{\partial t} + \vec{V} \nabla T \right) = \nabla(\lambda_i \nabla T) + P \quad (6)$$

Where the indices n and i correspond to the nature of the material (Copper, insulator, or semi-conductor).

$Q$ : Dissipated power (W/m<sup>2</sup>].

$T$ : Temperature [K].

$\rho_n, \rho_i$ : Density of the material [Kg / m<sup>3</sup>].

$Cp_n, Cp_i$ : Calorific capacity of material [J / Kg.k].

$K, \lambda_i$ : Thermal conductivity of the material [W/m.K].

$\vec{V}$ : Air speed if moving (convection) [m / s]

$t$ : Time [s]

$P$ : Source term corresponding to the generation of an internal heat flow [W/m<sup>3</sup>]

### 6.3 Thermal simulation

The thermal simulation makes it possible to envisage the temperature distribution in the different layers of the interleaved transformer. We worked with a stationary model, so the frequency was not taken into account.

First, we visualize the temperature distribution in the primary and secondary coils of our transformer (Fig. 12).

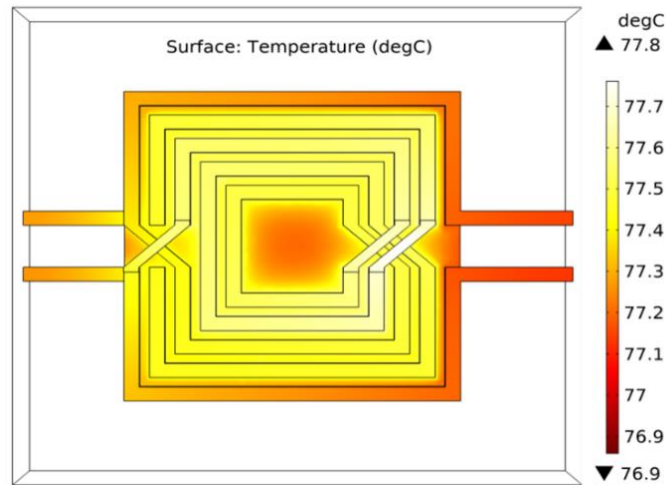


Fig.12.Temperature distribution in the primary and secondary coils.

Since our transformer does not have a core, only the joule losses are taken into account and contribute to the heating of the transformer. Fig. 12 shows a temperature varying between 76.9°C and 77.8°C in the primary and secondary coils. The operating transformer temperature is usually limited to below 120°C. therefore we can consider this temperature in the standards.

We observe that the temperature is evenly distributed inside the windings, this is due to the absence of the skin effect. The temperature of the secondary winding is slightly higher than that of the primary, because the current density of the secondary is slightly higher. We also notice that the external turn which is in contact with the air has the lower temperature, that confirms the presence of heat transfer by convection. The temperature curve in the windings (Fig. 13(b)) is plotted according to the cross section of Fig. 13(a).

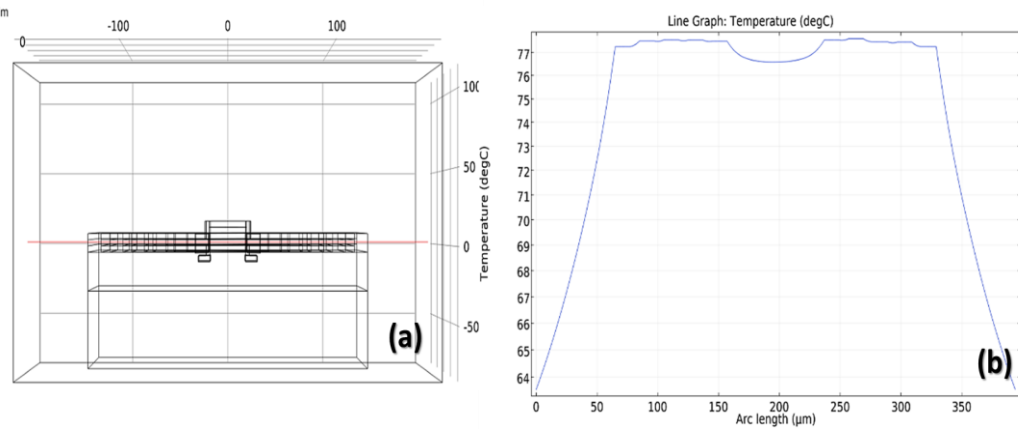


Fig.13. (a) Cross section, (b) Temperature curve in the primary and secondary coils

Fig. 13(b) reflects the same results of Fig. 12 and shows that the temperature at the center of the transformer is lower. This area is cooled by convection. Fig. 14(b) represents the temperature curve in the insulating silicon dioxide layer of the interleaved transformer. This curve is plotted according the cross section of Fig. 14(a).

The temperature of the primary and secondary coils is transferred by conduction to the insulating layer, and given the very low thickness of this layer (25 μm), there was no cooling during conduction, which shows a temperature of 77 °C throughout the insulating layer.

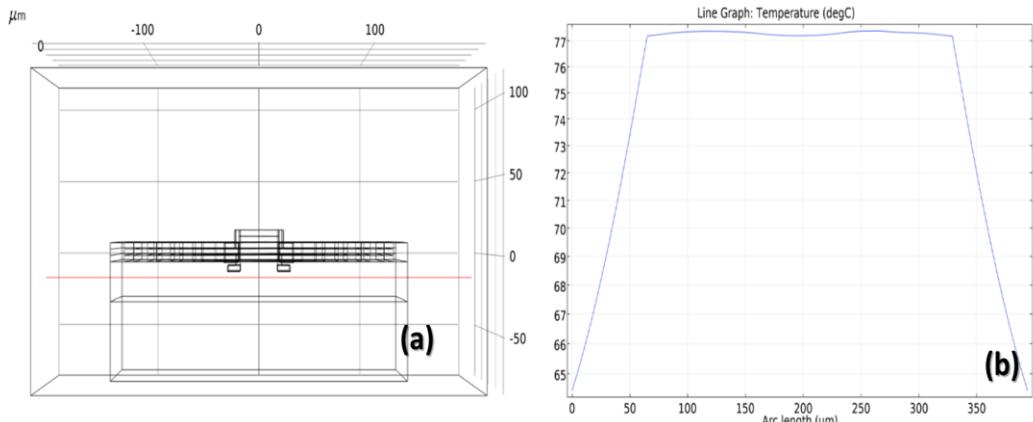


Fig.14. (a) Cross section, (b) Temperature curve in the insulating layer

The heat transfer by conduction does not stop in the insulating layer, but continues towards the semiconductor substrate (Fig. 15(b)) to reach a temperature of 77°C. The curve of Fig. 15(b) is plotted according to the cross section of Fig. 15(a).

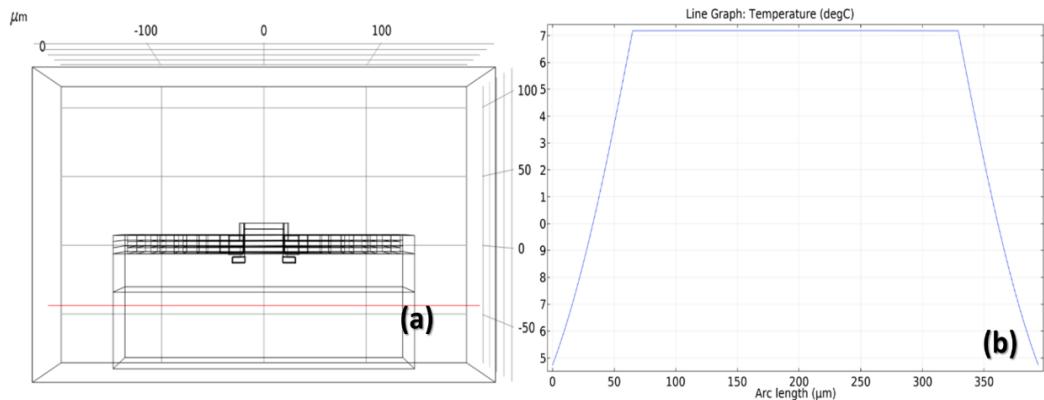


Fig.15. (a) Cross section, (b) Temperature curve in the substrate.

## 7. Conclusions

In this work, we studied the impact of the thickness of the substrate on the performance of an interlaced transformer. So we designed a symmetrical and interlaced transformer, with an outer diameter of 280 μm, a metal width of 20 μm and a thickness of 12 μm. We carried out different simulations in a frequency range of 1 MHz to 9 MHz in order to study the influence of the substrate thickness on the values of  $L_p$ ,  $R_p$ ,  $Q_p$  and the coupling coefficient. The simulation results have shown that a very thin substrate thickness (20 μm) degrades the performance of the transformer. Thicknesses between 100 μm and 150 μm have shown good behavior of the transformer. This study allowed us to optimize the substrate

thickness, but it remains insufficient if we do not treat the thermal effect. We therefore opted for a substrate thickness of 100 $\mu$ m, then we simulated the electromagnetic and thermal effects using the COMSOL Multiphysics simulation software.

The results showed good electromagnetic and thermal behavior of the interlaced transformer, with an acceptable current density and a temperature within the standards. We conclude that this study provided us with a guideline for optimizing substrate thickness for heat removal without affecting transformer performance.

## REFERE N C E S

- [1]. *Khan, Danial, et al.* "An efficient reconfigurable RF-DC converter with wide input power range for RF energy harvesting." *IEEE Access* 8 (2020): 79310-79318.
- [2]. *Dang, Kui, et al.* "Lateral GaN Schottky barrier diode for wireless high-power transfer application with high RF/DC conversion efficiency: From circuit construction and device technologies to system demonstration." *IEEE Transactions on Industrial Electronics* 67.8 (2019): 6597-6606.
- [3]. *A. Namoune, R. Taleb, A. Derrouazin, A. Belboula*, "Integrated Solenoid Inductor with Magnetic Core in a Buck Converter". *Przegląd elektrotechniczny*, Vol. 95, N°.8, pp 92-95, 2019.
- [4]. *Benzidane, Mohammed Ridha, et al.* "Miniaturization and Optimization of a DC-DC Boost Converter for Photovoltaic Application by Designing an Integrated Dual-Layer Inductor Model." *Transactions on Electrical and Electronic Materials* (2021): 1-14.
- [5] *Rack, Martin, Lucas Nyssens, and J-P. Raskin.* "Silicon-substrate enhancement technique enabling high quality integrated RF passives." *2019 IEEE MTT-S International Microwave Symposium (IMS)*. IEEE, 2019.
- [6] *Sepaintner, Felix, et al.* "Characterization and production of PCB structures with increased ratio of electromagnetic field in air." *IEEE Transactions on Microwave Theory and Techniques* 68.6 (2020): 2134-2143.
- [7] *Wang, Fengjuan, et al.* "A transformer with high coupling coefficient and small area based on TSV." *Integration* 81 (2021): 211-220.
- [8] *Mohd Yunus, Noor Hidayah, et al.* "Investigation of micromachined antenna substrates operating at 5 GHz for RF energy harvesting applications." *Micromachines* 10.2 (2019): 146.
- [9] *Xu, Pengcheng, Denis Flandre, and David Bol.* "Analysis, modeling, and design of a 2.45-GHz RF energy harvester for SWIPT IoT smart sensors." *IEEE Journal of Solid-State Circuits* 54.10 (2019): 2717-2729.
- [10] *Mumtaz, Farhan, et al.* "Review on non-isolated DC-DC converters and their control techniques for renewable energy applications." *Ain Shams Engineering Journal* 12.4 (2021): 3747-3763.
- [11] *Namoune A, Hamid A, Taleb R.* "the Performance of the Transformer for an Isolated DC/DC Converter". *TELKOMNIKA*. 2017. vol 15, No 3, pp. 1031-1039, September 2017.
- [12] *E. Macrelli, A. Romani, N. Wang, S. Roy, M. Hayes, R. Paganelli, C. O'Mathuna, M. Tartagni*, "Modeling, design, and fabrication of high inductance bond wire micro-transformers with toroidal ferrite core". *Power Electronics, IEEE Transactions on*, PP(99):1-1, 2014.

- [13] *S.J. Pan, W.Y. Yin et L.W. LI* : “Comparative investigation on various on-chip center-tapped interleaved transformers”. International Journal of RF and Microwave Computer-Aided Engineering, 14(5):424–432, 2004.
- [14] *Namoune A, Hamid A, Taleb R*. “Stacked transformer: influence of the geometrical and technological parameters”. International Journal of Engineering Research in Africa. 2015. vol 21, No 4, pp. 148-164, December 2015.
- [15] *O. El-Gharniti, E. Kerhervé, and J. B. Begueret*, “Modeling and Characterization of On-Chip Transformers for Silicon RFIC ”, IEEE Trans. Microw. Theory Techn., vol. 55, no. 4, pp. 607-615, Apr. 2007.
- [16] *B. Leite, E. Kerhervé, J.-B. Begueret, and D. Belot*, “An Analytical Broadband Model for Millimeter-Wave Transformers in Silicon Technologies”, IEEE Trans. Electron Devices, vol. 59, no. 3, pp. 582-589, Mar. 2012.
- [17] *Z. Gao, K. Kang, C. Zhao, Y. Wu, Y. Ban, L. Sun, W. Hong, Q. Xue*, “A broadband and equivalent-circuit model for millimeter-wave on-chip M:N six-port transformers and baluns”, IEEE Transactions on Microwave Theory and Techniques, Vol. 63, No. 10, pp. 3109–3121, 2015
- [18] *A. Namoune, A. Hamid and R. Taleb*, “Simulation analysis of geometrical parameters of monolithic on-chip transformers on silicon substrates”. Przegląd Elektrotechniczny, pp 253-257, 2017.
- [19] *H. C. Luong, J. Yin*, “Transformer-based design techniques for oscillators and frequency dividers”, Springer, 2016
- [20] *B. Chen, L. Shen, J. Gao*, “A 60 GHz transformer-coupled neutralized low power CMOS power amplifier”, Microwave and Optical Technology Letters, Vol. 57, No. 11, pp. 2487–2491, 2015
- [21] *S. Djuric, G. Stojanovic, M. Damnjanovic, M. Radovanovic, and E. Laboure*, “Design, modeling, and analysis of a compact planar transformer”, IEEE Trans. Magn., vol. 48, no. 11, pp. 4135–4138, Nov. 2012.
- [22] *Namoune A, Hamid A, Taleb R*. “Modeling and Structure Optimization of Tapped Transformer”. International Journal of Electrical and Computer Engineering. 2017. vol 7, No 1, pp. 41-49, February 2017.
- [23] *Dan Zhao, Kiat Seng Yeo, Manh Anh Do, Chirn Chye Boon*, “Characterization, design and modeling of on-chip interleaved transformers in CMOS RFICs”, Analog Integr Circ Sig Process (2011) 66:67–79
- [24] *V. N. R. Vanukuru*, “Highly efficient and symmetric stacked transformers for millimeter-wave ICS”, International Conference on Microelectronic Devices, Circuits and Systems, Vellore, India, August 10-12, 2017